Pergamon

Geochimica et Cosmochimica Acta, Vol. 67, No. 20, pp. 3803–3815, 2003

0016-7037/03 $30.00 + .00

doi:10.1016/S0016-7037(00)00270-9

Soil pore-water distributions and the temperature feedback of weathering in soils

PAUL L. RICHARDS* and LEE R. KUMP
Earth System Science Center, The Pennsylvania State University, University Park, PA 16802, USA

(*Received August* 8, 2002; *accepted in revised form January* 24, 2003)

Abstract—A review of the literature suggests that large variations in pore-water chemistry exist within soils. The heterogeneity indicates that in soil microchemical environments, the chemistry of pore water evolves independently from one pore to another due to differences in surface area/volume ratios and water residence time. A plug-flow reactor model was developed to examine which size classes of pores contribute the most solute to water draining out of the soil profile, and to explore how temperature might affect a soil's ability to generate solute. The model is based on the simplification that soil pores can be approximated as a suite of capillaries of varying diameter. The model simulates each size class of pores as a plug-flow reactor with an unique water residence time and surface area.

In the model, the pores which drain at the highest water contents have low surface area to water volume ratios and contribute relatively little to the overall solute flux from a soil. The smallest pores that drain at the lowest water contents were found to have the highest surface area to volume ratios and contribute the most solute. The calculations also suggest that activation energy and water viscosity have competing effects on the temperature dependence of weathering. As the temperature increases, the dissolution rate constant increases and smaller pores drain; however, water residence time decreases. This decrease in the water residence time is due to decreasing water viscosity, which can be incorporated into the dissolution rate law for quartz with an activation energy of approximately −15 kJ/mole. Studies that parameterize the temperature dependence of weathering using the Arrhenius approach can account for this effect by reducing the predicted activation energy by an appropriate value.

1. INTRODUCTION

An understanding of the environmental controls (e.g., surface temperature, rainfall distribution, vegetation and soil texture) that affect weathering fluxes are crucial if we are to model these controls in the present-day environment and in the past. Recent discussions have focused on the best way to parameterize the effect of temperature on global weathering rates (Brady, 1991; Velbel, 1993b; Brady and Carroll, 1994; White and Blum, 1995; Kump et al., 2000). The debate focuses primarily on the strength of the dependence of global weathering on temperature (Berner and Berner, 1997; Edmond and Huh, 1997), the significance of biologic mediation (e.g., Volk, 1987, 1989; Drever, 1994; Moulton et al., 2000), as well as the importance of uplift and physical weathering in keeping unweathered rock exposed (Edmond et al., 1995). Recent studies suggest that the effect that mean annual air temperature has on weathering fluxes can be modeled with an Arrhenius expression and that the activation energy can be compared to laboratory activation energies. While this relationship has the advantage of simplicity and has also been demonstrated to be appropriate for modeling dissolution rates in the laboratory, it assumes that the effect of temperature on weathering is entirely chemical and that no physical parameters (e.g., surface area, water residence time) are affected by temperature. Several authors have pointed out that observed field estimates of mineral dissolution rates are slower than laboratory estimates (reviewed in Brantley, 1992; White and Brantley, 1995) and that some of the discrepancy must be due to differences in flow characteristics between field and laboratory systems (Swoboda-Coburg and Drever, 1993; Velbel, 1993a). The flux of solute that leaves the soil profile and becomes a part of the total flux of solute leaving a watershed (i.e., the chemical erosion rate) is also not known. Clearly a temperature feedback of weathering fluxes will have to include any effect temperature might have on the ability of rain to flush "old water" out of the weathering profile. It is interesting to note that in a study comparing basalt weathering in Iceland and Hawaii, Bluth and Kump (1994) found that chemical erosion rates were faster in Iceland, despite the fact that Iceland is cooler. Bluth and Kump (1994) interpreted this behavior to be due to differences between the thickness and structure of soils at the two locations. Hawaiian soils are in general thicker, and percolating soil water has less access to fresh rock than in Iceland. Brady (1991), Brady and Carroll (1994) and White and Blum (1995) admit that there exist a number of pedogenic factors that determine weathering rates in soils and that these factors are probably interrelated and are influenced by mean annual temperature in a complex way. The goal of our study is to take a next step in exploring the nature of the coupling between temperature and weathering by considering some of the effects that temperature has both on reaction kinetics and on water mobility in soils.

In this paper we conjecture that some of the water in a soil profile has an exceedingly long residence time. The chemistry of water within the soil, therefore, may be considerably different than the chemistry of the water draining from the soil profile and leaving watersheds in rivers and streams. The evidence for a high degree of chemical variation in moisture within the same kind of soil is used to support the hypothesis that weathering processes are not uniform in a soil, and that soil

* Author to whom correspondence should be addressed, at School of Natural Resources and the Environment, Dana Building, 430 East University, University of Michigan, Ann Arbor, MI 48109-1115, USA (pauljr@umich.edu).

water chemistry varies with the size of the pore. The overall weathering flux from a soil is therefore controlled by the size classes of pores that drain. Using the soil physics paradigm of simulating soil pores as capillary tubes, we have created a geochemical dissolution model to explore the effect temperature has on weathering fluxes. The model includes the effect that temperature has in controlling which size classes of pores drain. While the model is simplistic, it enables us to estimate surface area to volume ratios and residence times for individual water packets moving through the soil, enabling estimation of weathering fluxes incorporating both reaction kinetics and flow pathways.

2. FIELD AND THEORETICAL CONSIDERATIONS

2.1. Spatial Variability of Soil Water Chemistry

The evidence supporting a large spatial variation of soil water chemistry comes from two sources: 1) studies describing soil pore-water chemistry in which large variations of soil moisture chemistry were observed within "uniform" soils (Haines et al., 1982; Starr, 1985; Richter and Jury, 1986; Ugolini et al., 1988; Campbell et al., 1989; Grieve, 1990; Swistock et al., 1990; Zabowski and Ugolini, 1990; Denning et al., 1991; Hendershot and Courchesne, 1991; Arthur and Fahey, 1993; Giesler and Lundstrom, 1993; Quisenberry et al., 1994; Johnson, 1996); and 2) field studies of through-flow chemistry that document large variations in chemistry between different kinds of soil pores (Cozarelli et al., 1987; Parnell, 1993; Swoboda-Coburg and Drever, 1993).

Campbell et al. (1989) analyzed pore-water samples from woodland soils in Oxfordshire, England and observed that for solutes like K, S, Si, and P, variance among samples taken within the same soil exceeded the variance among different soils. They found that Ca and Si showed the smallest range of concentrations and interpreted this to be caused by precipitation of secondary minerals containing these elements. A study by Kazda and Katszensteiner (1993) showed that ion concentrations in soil water are positively correlated with matric potential. This observation is consistent with the popular interpretation that water held more tightly to a soil has been present in the soil for a longer period of time, and as a consequence has a higher solute concentration. In a study investigating seasonal mineral stability in soils, Zabowski and Ugolini (1992) observed that water extracted from soil samples with a centrifuge was chemically different than water samples obtained from tension lysimeters. The authors concluded that the centrifuged samples are releasing water that is more strongly held within micropores. Such water will have higher concentrations of dissolved solute because it has spent more time in contact with grain surfaces. Zabowski and Ugolini (1992) centrifuged some samples at pressures exceeding 30 kPa. Water left behind in these samples cannot percolate through a soil because matric forces far exceed the gravitational forces driving the water out. Other authors (Swistock et al., 1990; Denning et al., 1991; Magid and Christensen, 1993; Giesler et al., 1996) have postulated that tension lysimeters, relative to pan lysimeters, sample micropore regions preferentially. Hendershot and Courchesne (1991) observed that cation concentrations in tension lysimeters were higher than concentrations in pan lysimeters at 25 cm soil depth. Solution chemistry from both kinds of collection devices was similar at 75 cm depth. While the latter observation is not entirely consistent with the notion that tension lysimeters preferentially sample water from micropores, Hendershot and Courchesne (1991) observed that a compacted soil horizon characterized by low permeability existed at 75 cm of depth. Such a horizon encourages ponding, and the similarity in chemistry between tension and pan lysimeters may in fact be because the source of water was the same for both devices in the studied soil.

In addition to this direct evidence for chemical variation in soils, there is abundant evidence for spatial heterogeneity in soil characteristics that determine water mobility. De Vries and Chow (1978) placed an array of tensiometers in a forested mountain soil and discovered that significant spatial and temporal variations in matric potential occurred during infiltration. They interpreted this variation to indicate that water is flowing through macropores at different times during the course of infiltration. Soil scientists have long noted that hydraulic conductivity is log-normally distributed (Jury et al., 1991) and that saturated hydraulic conductivity can vary considerably within a uniform soil (Nielsen et al., 1973; Lauren et al., 1988; Schoeneberger and Amoozegar, 1990; Jabro et al., 1991a; Vepraskas et al., 1996). The origin of this variation is undoubtedly the variability in size and geometry of pores that have been observed in soils (Bouma and Dekker, 1978; Luxmoore, 1980; Beven and Germann, 1981, 1982; Germann and Beven, 1981; Wilson et al., 1990). Studies of fluid flow in some of these soils (Bouma et al., 1977; Ligon et al., 1980; Flury et al., 1994). Since the extent of dissolution is controlled in part by water residence time, we would expect that the rate of weathering will also vary between pores. Field studies (Russell and Ewel, 1985; Arthur and Fahey, 1993; Giesler et al., 1996; Johnson, 1996) commonly observe that volumes of water collected by nearby lysimeters vary, despite the fact that the lysimeters sample the same depth and collect water over the same period. Arthur and Fahey (1993) interpret this as evidence of the existence of preferential flow paths.

All this evidence suggests that microchemical environments exist within soils in which the chemistry of the individual waters can evolve independently from one another. The reason for this spatial variability in chemistry is, among other factors, the spatial heterogeneity in soil structure which causes water residence time and susceptibility to evaporation to vary over short distances. One then needs to consider which of these microchemical environments are actively draining during the course of an infiltration and percolation event, and which of these soil microenvironments are the most important contributors to weathering fluxes at the scale of interest. Finally, in scaling upward from soils to watersheds, the effect of temperature on microenvironment drainage must also be considered.

2.2. Temperature Dependence of Solute Transfer

Temperature will affect a soil's release of solutes by modifying surface tension, water viscosity, dissolution rate, diffusion rate and equilibrium constants of the minerals present. In addition, biologic activity will also be affected by temperature. Surface tension forces at the water, mineral, and gas interfaces contribute to the forces that hold water in the micropores.

Consequently, a change in surface tension due to temperature will change the size classes of micropores that can drain. Experimental studies of the temperature dependence of water retention curves (Richards and Weaver, 1944; Gardner, 1955; Wilkinson and Klute, 1962; Haridasan and Jensen, 1972; Hopmans and Dane, 1985, 1986) document a strong dependence of temperature on a soil's ability to hold water that is thought to be due to surface tension and the equilibrium size of gas bubbles (Peck, 1960; Chahal, 1965). Laboratory studies of surface tension indicate that surface tension decreases with increasing temperature; consequently, we might hypothesize that increases in temperature will allow smaller micropores to drain.

Water viscosity, a function of temperature, influences hydraulic conductivity (Childs, 1964; Haridasan and Jensen, 1972; Freeze and Cherry, 1979). Consequently, variations in temperature will cause variations in water residence time of the micropores, thus affecting the total solute load for the water when it finally drains out of the soil profile. Since the viscosity of water decreases with increasing temperature, we would expect water residence time to decrease with increasing temperature.

At the water-rock interface, temperature influences dissolution by influencing the rate constant and the equilibrium constant. The activation energy describes the effects of temperature on the forward rate constant. It is related to the potential energy barrier associated with the reaction of the activated complex of the rate limiting step (Lasaga, 1981; Laidler, 1987). The higher the activation energy, the stronger the temperature dependence of the dissolution reaction. Moreover, laboratory studies of water-rock interaction show that net dissolution reactions slow down as equilibrium is approached. The temperature dependence of the equilibrium constant will thus affect the weathering flux for some minerals.

2.3. Significance of Matric Potential and Observed Soil Water Distribution

Matric potential is the potential energy of water in the soil created by forces that tend to hold water to the soil. These matric forces include surface tension, adsorptive forces, osmotic forces and Van der Waals forces (Wilkinson and Klute, 1962). The strength of these forces is strongly influenced by the interfacial area of the water-grain contact in the pores. These forces may also influence the driving force for the reaction (Mercury and Tardy, 2001). Since the size (a proxy for the interfacial surface area) and distribution of pores varies considerably spatially (see Velbel, 1993a, for a review) the strength of these forces will also vary spatially. A consequence of this is that water will drain first out of those pores where matric forces are weakest i.e., the largest macropores, since the ratio of their surface area to water volume are the lowest. As the soil drains, water is released from smaller pores and thinner films within large pores. In some pores, water is so tightly held that the water may never drain. In addition, a water film coats all mineral surfaces even at great aridity.

One way of visualizing this relationship for a particular soil is through a water retention curve (Jury et al., 1991). A water retention curve is a plot of matric potential versus the water content of the soil. The curve can reveal the amount of water held in the soil at or above a certain matric potential. Because correlation between the size of the pore and the matric potential can be assumed, a water retention curve also provides information on the size of the pore that drains at a particular water content (Childs and Collis-George, 1950).

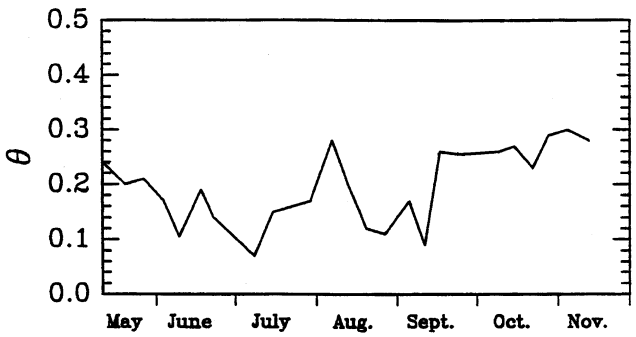

Fig. 1. Fractional water content (θ), of a Leck Kill silt loam in Pennsylvania, United States, over the growing season. The local increases are due to rainfall events. After Henninger (1972).

Field studies of soil moisture variability (Henninger, 1972; Rogowski et al., 1974) demonstrate that water content fluctuates with rainfall and season. For many soils in the humid temperate northeast U.S., for example, water content will only drop below field capacity (the water content of the soil at which drainage is imperceptible) during the growing season, when evapotranspiration is active (Fig. 1). This seasonal minimum water content, if compared to a water retention curve appropriate for the soil, indicates the size classes of pores in the soil that drain imperceptibly slowly according to the Childs and Collis-George model. Solutes released by weathering within these pores will only leave the soil by diffusion into pores that do drain (Thomas and Phillips, 1979; Swoboda-Coburg and Drever, 1993).

This observation leads to some pertinent questions: 1) What percentage of the total surface area in a soil defines pores that cannot drain? 2) What fraction of the solutes released by the soil are contributed from weathering within pores that do drain? The difference between the total amount of solute flowing out of a soil and the amount contributed by drainable pores has to be due to diffusion of solute from the parts of the soil that never drain. 3) How might temperature affect the size classes of pores that drain? In what follows, these questions are explored using a plug-flow-reactor model of weathering in soils, which incorporates the capillary model of soil porosity.

3. WEATHERING MODEL

3.1. Structure and Movement of Water in Soils

Early descriptions of the geometry of water in the unsaturated zone (Haines, 1927, 1929; Baver, 1938; Nelson and Baver, 1940) come from observations taken from experiments in which well rounded, uniform, ideally packed grains were repeatedly saturated and dried. Even in simple packing systems, water exists in a continuum of complex shapes that can change considerably during wetting and drying. Stallman (1964) reviews some of this early work and summarizes the changes that water undergoes during the process of draining from an initially

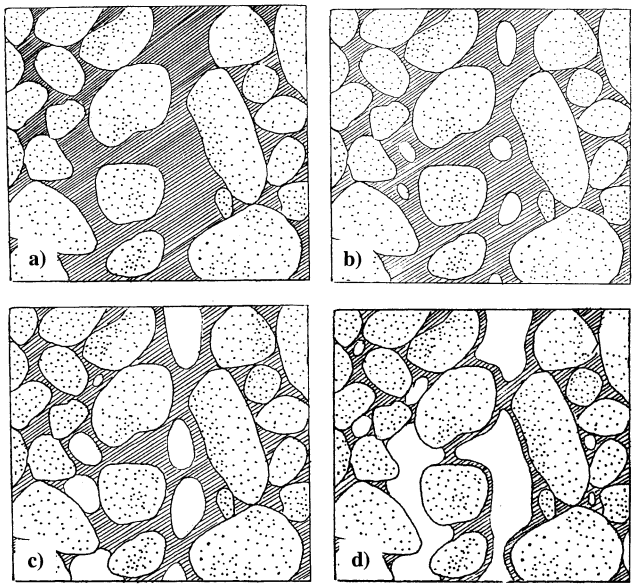

Fig. 2. Sketch showing the changes in water geometry that occur during drainage. Note as the films of water get progressively thinner, the surface area to volume ratio increases.

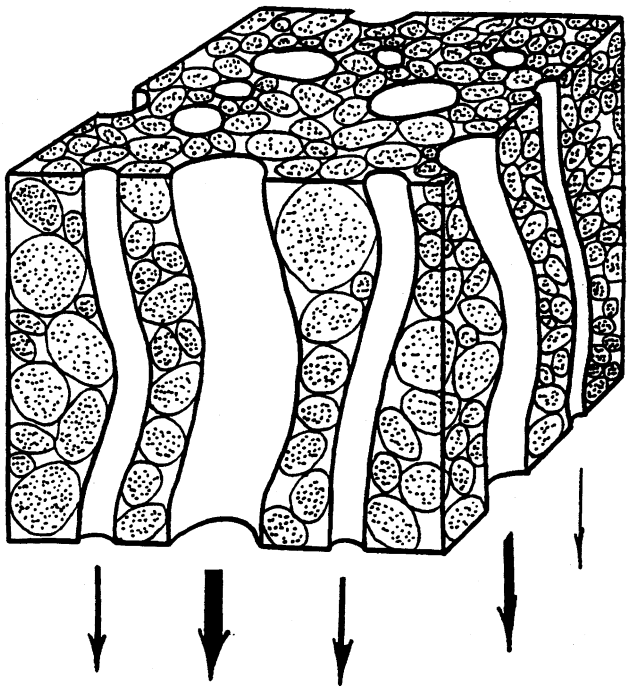

Fig. 3. Conceptual view of soil porosity as through-going cylindrical pores. weathering will be simulated in this paper by treating each pore as a plug-flow reactor with a unique surface area and water residence time.

saturated state (Fig. 2). As drainage begins, bubbles form in the center of pore spaces and water drains along thin films adjacent to grain surfaces. The bubbles increase in size until grain surfaces are covered by thin films of water. Further dewatering decreases the thickness of the water films. Water may also be drawn laterally into smaller pores in response to matric potential gradients (Horton and Hawkins, 1965). Eventually, water is restricted to small bridges (menisci) located at points of grain contact, at which drainage ceases. These observations indicate that the surface area to volume ratio of water in the pore space increases during the drainage cycle. Solute transfer models ought to approximate these changes.

3.2. The Model

The premise for the model is that the flow paths described above can be represented as bundles of capillary tubes of various diameters that drain at particular matric potentials (Fig. 3). In the model, we assume that every class of micropore

and macropore in a soil can be approximated as a plug flow reactor (with specific surface area to volume ratios and water residence times) operating concurrently. This approach simulates both the increase in surface area to volume ratio that occurs during drainage and simulates the observation that water in smaller pores is more tightly held. Furthermore, the model allows the use of a frequently measured soil property (the matric potential-water content curve) to develop a simplified porous geometry that is amenable to solute-transfer calculations. While such a model is simplistic in that pores are treated as noninteracting tubes of constant diameter, the model is useful as a first step in understanding some of the coupling between flow path and solute chemistry.

This idea for modelling soil originated from Childs and Collis-George (1950) and was used to derive a relationship between hydraulic conductivity and soil moisture content. The model was later modified by Marshall (1958), and has been shown to be useful in predicting unsaturated hydraulic conductivity in particular soil textures. Using the model, the solute flux out of the soil profile is the total solute contributed by all the size classes of pores that have completely drained per unit time.

As a first attempt to understand predictions of the model, we assume that all pores are initially saturated and that pores drain concurrently, though at variable rates. The flux can be approximated by dividing the total solute contributed by all the pores that drain by the period of time between rainfall (saturation) events. Model calculations occur in three steps: 1) calculation of the size and number of capillaries that simulate the water retention curve of a particular soil texture; 2) determination of which of the pores would drain if the initially saturated soil were allowed to drain to a particular matric potential; and 3) calculation of the amount of solute generated by each class of micropore using plug flow reactor theory and the general rate law of Lasaga (1984).

3.3. Determination of the Size and Number of Capillaries that Make Up a Soil

The following treatment of the Childs and Collins-George model follows Jury et al. (1991). A matric potential (H; cm of water) vs. water content (θ) graph (Fig. 4) is divided into equal fractional water content intervals ($\Delta\theta$). The maximum matric potential (H_j) for each water content interval is obtained from the graph. The radius of the capillary (r_j) at which the matric potential exactly balances the surface tension forces retaining the water is calculated using a form of the Laplace Eqn. 1:

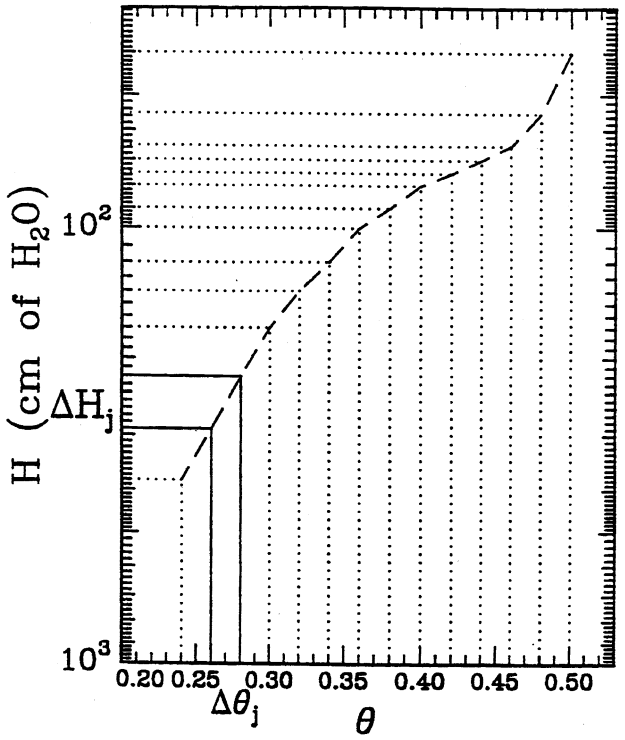

Fig. 4. Matric potential (ΔH) plotted against fractional water content (θ) for the silt loam example. In the Childs and Collis-George (1950) model, the curve is subdivided into equal water content intervals and the maximum matric potential is obtained for each.

$$r_j = \frac{2\sigma}{\rho g \Delta H_j} \tag{1}$$

where σ is the surface tension of water in g/s^2, ρ is the density of water in g/cm^3, and g is the acceleration of gravity in cm/s^2. To parameterize σ as a function of temperature (T) we obtained surface tension data for pure water in contact with air from Weast and Melvin (1979) from 0° to 30°C and applied a Taylor polynomial curve fit. Eqn. 2 was found to adequately characterize the data over the temperature range ($R^2 = 0.9996$):

$$\sigma = 78.617 + 0.112T - 0.00045T^2 \tag{2}$$

To determine the number of capillaries of radius r_j that empty for a change in water content ($\Delta\theta$) we divide $\Delta\theta$ by the volume of the capillary (3),

$$n_j = \frac{\Delta\theta}{\pi r_j^2 L} \tag{3}$$

where n_j is the number of capillaries of radius r_j and L is the thickness of the saturated layer (cm) in the soil. Eqns. 1, 2 and 3 are evaluated for every interval j.

3.4. Calculation of the Solute Generated by Each Size Class of Pore

To estimate the total solute contributed by dissolution of phases in each class of capillary we evaluate a modification of the general rate law discussed by Lasaga (1984):

$$M = K_t A_r \tau_{t,r} \Omega_{t,r} \tag{4}$$

Here M is the total number of moles of solute produced; K_t is the rate constant for the reaction in mol/cm^2/s, a function of temperature; A_r is the surface area of the capillary in cm^2, a function of the radius of the capillary and the roughness coefficient; $\tau_{t,r}$ is the water residence time of the capillary in seconds, a function of temperature and the radius of the capillary; $\Omega_{t,r}$ is the affinity term, a dimensionless function modifying the rate law for the chemical saturation state with respect to the dissolving mineral in the capillary. Conspicuously missing from Eqn. 4 are terms describing the effect of pH on the rate law and the effect of catalysts and inhibitors that may be present in the capillary. These terms have been shown to be very important in dissolution studies of minerals (e.g., Chou and Wollast, 1984; Helgeson et al., 1984; White and Brantley, 1995) but are assumed in this study for the sake of simplicity to be incorporated into the rate constant. Rate constants are chosen for a pH value of 5. K_t is evaluated using the integrated form of the Ahrrenius equation e.g., (Velbel, 1990):

$$K_t = K_{ref} \exp\left\{\frac{E_a (T_{ref} - T)}{RT_{ref}T}\right\} \tag{5}$$

Where K_{ref} is the reaction rate at the reference temperature (298°K) in mole/cm^2/s, E_a is the activation energy in cal/mole, T_{ref} is the reference temperature in K, T is the temperature of interest in K, and R is the gas constant in cal/K/mole. The reactive surface area of the capillary is assumed to be the geometric surface area of the cylindrical capillary multiplied by a dimensionless roughness coefficient λ (White and Petersen, 1990):

$$A_r = 2\pi r L \lambda \tag{6}$$

Because soils have pores that are complex and vary greatly in size, the geometric surface area of the cylindrical capillary that approximates the pore will underestimate the reactive surface area along the flow path. The purpose of the roughness coefficient is to provide a mathematical way to account for this missing surface area. λ is commonly evaluated for mineral grains by dividing the surface area determined with BET to the surface area determined with geometric considerations (White and Petersen, 1990). For naturally weathered minerals, λ can range from 1.08 to 2600; see Anbeek (1992) for a review. In this study, calculations will be repeated for a range of λ to see how sensitive the temperature feedback is to uncertainty in reactive surface area. Water residence time is calculated by dividing the volume of the entire cylindrical capillary (Eqn. 7) by the flux at steady state. Because the Childs and Collis-George (1950) model assumes that flow in capillaries is laminar, Pouseille's law can be used to calculate the flux out of the capillary:

$$V = \pi r_j^2 L \tag{7}$$

$$Q_c = \frac{\pi r^4 \rho g \Delta H_j}{8\upsilon L} \tag{8}$$

Here V is the volume of the capillary in cm^3, Q_c is the flux in cm^3/s, ΔH_j is the energy (per unit weight) of the water in the capillary in cm, and &rtf-symbol-117; is the coefficient of

Table 1. Calculated pore sizes and distribution for Dubb's silt loam.

j	θ	$\Delta\theta$	Hj (cm)	ΔH_j (cm)	σ	r_j (cm)	L (cm)	n_j
0	0.52							
1	0.5	0.02	40	60	72.0312	0.001322	100	36.4
2	0.48	0.02	55	45	72.0312	0.000961	100	68.8
3	0.46	0.02	65	35	72.0312	0.000814	100	96.1
4	0.44	0.02	70	30	72.0312	0.000756	100	111.5
5	0.42	0.02	75	25	72.0312	0.000705	100	128.0
6	0.4	0.02	80	20	72.0312	0.000661	100	145.6
7	0.38	0.02	90	10	72.0312	0.000588	100	184.3
8	0.36	0.02	100	0	72.0312	0.000528	100	227.6
9	0.34	0.02	120	−20	72.0312	0.000441	100	327.7
10	0.32	0.02	140	−40	72.0312	0.000378	100	446.0
11	0.3	0.02	170	−70	72.0312	0.000311	100	657.7
12	0.28	0.02	220	−120	72.0312	0.000240	100	1101.4
13	0.26	0.02	290	−190	72.0312	0.000182	100	1913.8
14	0.24	0.02	380	−280	72.0312	0.000139	100	3286.0

dynamic viscosity in g/cm/s. ΔH_j can be determined by subtracting the gravitational potential energy of water from the surface tension energy tending to hold the water in the capillary. For large pores where surface tension is negligible, the hydraulic gradient (ΔH_j /L) will be 1. For smaller pores, the hydraulic gradient will be less then one. Dividing Eqn. 7 by Eqn. 8 yields the residence time for the capillary (Eqn. 9).

$$\tau_{t,r} = \frac{8\upsilon L^2}{r^2 \rho g \Delta H_j} \tag{9}$$

To parameterize dynamic viscosity as a function of temperature, we obtained water viscosity data from Weast and Melvin (1979) and applied a Taylor polynomial curve fit. A second-order curve fit was found to be adequate to characterize the data ($R^2 = 0.9994$):

$$\upsilon = 0.674 + 0.004T + 6.87 \times 10^{-6}T^2 \tag{10}$$

This same set of data could also be characterized with an Arrhenius parameterization with an activation energy of ~18 kJ/mole (Velbel, personal communication). ΔH_j/L is the affinity term that modifies the rate constant as equilibrium is approached. This term will vary with the mineral dissolved but we assume the form of Eqn. 11, modified from Nagy et al. (1991),

$$\Omega_{t,r} = \left(1 - \exp\left(A \ln\left(\frac{Q}{K_{eq}}\right)^B\right)\right) \tag{11}$$

where Q is the ion activity product and K_{eq} is the equilibrium constant, a function of temperature. The parameters A and B are empirically obtained coefficients used to fit the affinity equation derived from transition state theory (Lasaga, 1981) to observed dissolution rate versus ΔG_r data; see Burch et al. (1993) for an example. The values and sources of these constants will be explained below.

To model K_{eq} as a function of temperature, we used the integrated form of the Van't Hoff equation (Stumm and Morgan, 1982),

$$K_{eq_t} = K_{eq_{ref}} \exp\left\{\frac{\Delta H_r(T_{ref} - T)}{RT_{ref}T}\right\} \tag{12}$$

where K_{eqref} is the equilibrium constant at the temperature of reference (25°C) and ΔH_r is the enthalpy of reaction. Eqn. 12 substituted for K_{eq} in Eqn. 11 gives an expression for $\Omega_{t,r}$ that is a function of temperature and the saturation state of the capillary:

$$\Omega_{t,r} = \left(1 - \exp\left(A \ln\left(\frac{Q}{K_{eq_{ref}} \exp\left(\frac{\Delta H_r(T_{ref} - T)}{RT_{ref}T}\right)}\right)^B\right)\right) \tag{13}$$

The final equation for mass of solute accumulated in the capillary over some time interval is obtained by substituting Eqns. 5, 6, 9 and 13 in Eqn. 4:

$$M = K_{ref} \exp\left(\frac{Ea(T_{ref} - T)}{RT_{ref}T}\right) \frac{16\pi\nu L^3 \lambda}{r\rho g \Delta H} \left(1 - \exp\left(A \ln\left(\frac{Q}{Keq_{ref} \exp\left(\frac{\Delta H_r (T_{ref} - T)}{RT_{ref}T}\right)}\right)^B\right)\right) \tag{14}$$

3.5. Soil Textures and Conditions Modeled in This Study

Water retention data were obtained for a silt loam (Haridasan and Jensen, 1972) and a sand (Jury et al., 1991). Figure 4 shows the water retention curve for the silt loam. The curve was divided into intervals of $\Delta\theta$ equal to 0.02 and Eqns. 1 and 3 were solved for a variety of temperatures to calculate the size (radius) and number of pores that drained during each incremental drop of water content. The results of these calculations are presented in Tables 1 and 2 (for silt loam and sand respectively; 298°K).

4. RESULTS

4.1. What Pores Have the Greatest Surface Area and Do They Drain?

To determine the portion of the water retention curve where the surface area per unit volume is the largest, we solved Eqn. 6 for each $\Delta\theta_r$ interval in the water retention curve. Total drainable surface area (A_{tot}) for the soil is calculated by sum-

Table 2. Calculated pore sizes and distributions for a sand textural class.

j	θ	$\Delta\theta$	Hj (cm)	ΔHj (cm)	σ	r_j (cm)	L (cm)	n_j
0	0.4							
1	0.35	0.05	13	0.87	72.0312	0.007707	100	2.68
2	0.3	0.05	27	0.73	72.0312	0.003711	100	11.56
3	0.25	0.05	47	0.53	72.0312	0.002132	100	35.02
4	0.15	0.05	148	−0.48	72.0312	0.000677	100	347.26
5	0.1	0.05	345	−2.45	72.0312	0.000290	100	1886.98

ming the surface area for all $\Delta\theta_r$ from saturation to "dryness" at 298 K:

$$A_{tot} = \sum_{rat\theta = Sat.}^{rat\theta = Dry} n_r A_r \qquad (17)$$

Note that this is a conservative estimate of the total surface area of the soil since it does not include the surface area of pores smaller than the smallest pores calculated in Table 1. Figures 5A,B show the surface area of the soil that drained when the pores in that water content interval drained for the silt loam and sand respectively. The calculations suggest that pores in the silt loam that drained when the soil water content dropped from saturation (0.50) to (0.35) contain only a small fraction of the total surface area of the soil. A silt loam that has a water content that stays above 0.35, not uncommon for the period between late fall and spring in the humid northeast (Henninger, 1972), will be draining water that has relatively little contact with mineral surface area compared to water retained in the smallest pores. Below 0.35 the pores that drain have significantly more surface area per unit volume. Figures 5A,B also show a similar curve calculated for 0°C. As hypothesized, warmer waters do

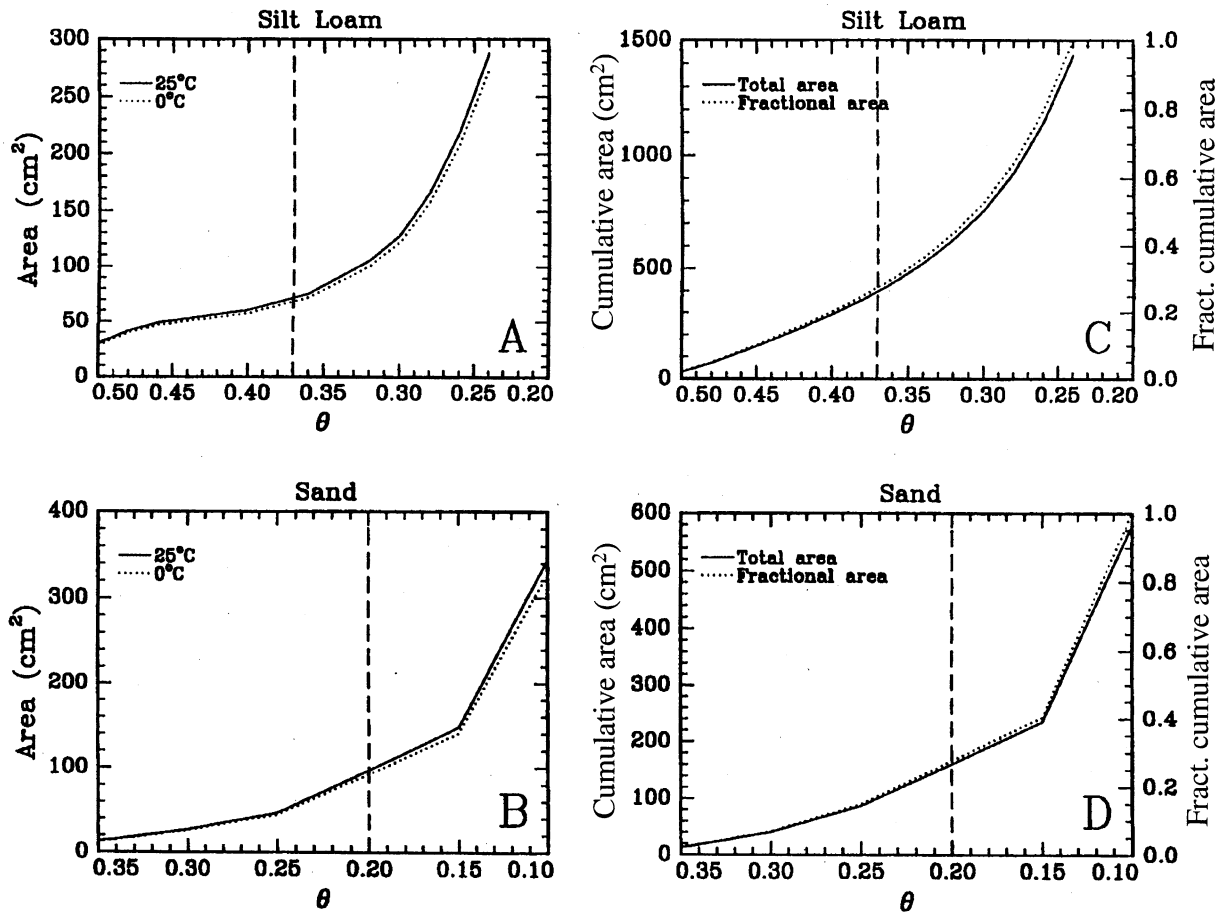

Fig. 5. Surface area and cumulative area exposed in pores that drain in a particular water content interval. The vertical dashed lines denote the critical water content at which pores cannot drain (i.e., when the gravitational energy of the water exactly balances surface tension energy holding the water to the pore). All calculations were carried out with a roughness of 1 and a length of 100 cm. The solid and dashed lines are the calculations for 25 and 0°C respectively.

drain greater surface area, but the effect is very slight because of the small dependence of surface tension on temperature between 0°C and 25°C.

Figures 5C,D present the cumulative fractional surface area of the soil that drained at a particular water content for the silt loam and sand respectively. Only when the volumetric water content has dropped to 0.30 has 50% of the total surface area of the silt loam drained. The last 0.10 drop in soil moisture content drains the rest of the total drainable surface area. For the sand, the lowest volumetric water content it can drain to theoretically (0.2) only exposes 25% of the cumulative fractional area. It is apparent that for both soil textures to release the water that is in contact with the bulk of the mineral surface area, the soil has to drain to very low (sometimes impossibly low) water contents.

4.2. Water Residence Time

Eqn. 9 was solved for all $\Delta\theta_r$ with a saturated thickness (L) of 100 cm to determine the amount of time required for the pores draining at each $\Delta\theta_r$ to drain completely (Figs. 6A,B). The graph shows the time required to drain the size class of pores that drain at a particular water content. The calculation assumes the pores were fully saturated initially. The curves in Figure 6 suggest that water residence time is sensitive to temperature; with decreasing temperature the water residence time increases. The magnitude of this effect (Fig. 6B) showing a near doubling of water residence time in all size classes of pores as the temperature is decreased from 25 to 0°C. Inspection of Eqn. 9 suggests that $T_r \alpha L^2$. Water residence time is thus very dependent on the length of the pore. Since Eqn. 14 was solved with a uniform L for all size classes of pores, it is possible that some error is introduced in the water residence time evaluation because L probably varies with the size of the pore.

4.3. Solute Generation as a Function of Pore Size

Solute calculations were calculated for the dissolution of quartz and kaolinite in the sand and silt loam textural classes. Tables 3 and 4 present the kinetic constants used. The total amount of solute per unit volume generated by pores draining at a particular water content was calculated to determine at what water content most of the solute was released (Fig. 7). For the silt loam and sand textural classes, pores that drained at the lowest water contents produced the greatest amount of solute per unit volume. For the sand example (Fig. 7B) pores draining at a water content of 0.1 generated 800 times more solute per unit volume than pores draining at field saturation ($\theta = 0.35$).

Increasing temperature increases the solute produced by the pores. This effect is due primarily to the temperature effect on the rate constant (activation energy). The magnitude of the effect is highest with quartz (11 times more solute at 25°C then at 0°C) and barely noticeable for kaolinite (Figs. 7C,D). It is important to note that this temperature effect is smaller than what is predicted by only modifying the rate constant with the Arrhenius equation and calculating the solute produced. The reason is that as temperature increases, water residence time decreases, reducing water mineral contact time. For quartz, 30 times more dissolved silica is generated at 25°C than 0°C (for pores draining at a water content of 0.35) when the temperature

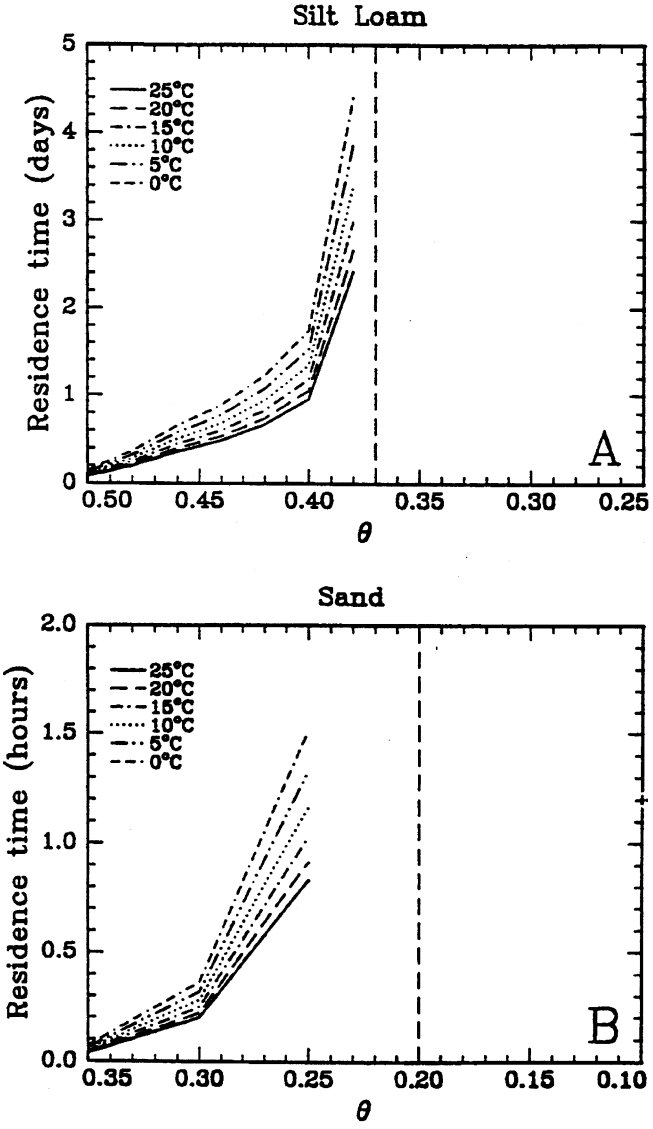

Fig. 6. Water residence time for pores that at the particular water content interval for a silt loam (A) and a sand (B). Calculated with Eqn. 9 and a length of 100 cm. Notice the strong dependence on temperature.

effect on water residence time is not included and only 17 times when it is included. In comparison, twice as much dissolved solute is produced at 25°C than at 0°C from kaolinite when the temperature effect on water residence time is not included, and only 20% more when it is included. For kaolinite dissolution,

Table 3. Conditions for the dissolution of kaolinite example.

Variable	Value	Reference
K_t	10^{-17} moles/cm^2/sec	Carroll and Walther (1990)
Ea	20.5 kJ/mole	Carroll and Walther (1990)
T_{ref}	298 K	Carroll and Walther (1990)
R	8.314 kJ/deg/mole	Stumm and Morgan (1982)
L	100 cms	
λ	1, 5, 10	

Table 4. Conditions for the dissolution of quartz example.

Variable	Value	Reference
K_t	10^{-17} mole/cm^2/sec	Rimstidt and Barnes (1980)
E_a	91.2 kJ/mole	Knauss and Wolery (1986)
T_{ref}	298 K	Rimstidt and Barnes (1980)
R	8.314 kJ/deg/mole	Stumm and Morgan (1982)
L	100, 200, 300 cms	
λ	1, 5, 10	

consideration of the temperature effect on residence time is even more important since its dissolution reaction has a lower activation energy. We can calculate an apparent activation energy correction that describes the effect that water viscosity and surface tension have on the temperature dependence of the model by solving Eqn. 5 for activation energy and substituting K_t with an effective K_t found by dividing the solute produced by the model at the temperature of interest with the surface area and water residence time of the pores at the reference temperature. Solving this for the temperature variation between 25°C and 0°C yields an activation energy of −15 kJ/mole. Thus, the apparent activation energy that should be used to account for the temperature feedback on weathering is 15 kJ/mole less than the activation energy of the laboratory rate constant for the 0 to 25°C interval.

Calculated cumulative solute production for all the pores that have emptied at a particular water content (Fig. 8) suggests that the bulk of the solute is released by the draining of the lowest water contents. For the silt loam example, draining from field saturation (0.5) to 0.27 releases 50% of the total solute that could be produced. Subsequent draining from only 0.27 to 0.25 releases the other 50%. The importance of smaller pores is due to the high surface area and long residence times associated with them.

5. DISCUSSION

The model calculations presented here suggest that the highest surface area to volume ratios and greatest solute production are associated with pores that drain only at high matric potentials. This aspect of the soil system makes it important to quantify the mechanisms (diffusion, advection) that are capable of moving solute to pores that drain at low matric potentials. Undoubtedly some of the discrepancy between field and laboratory rates of weathering comes from an underappreciation of

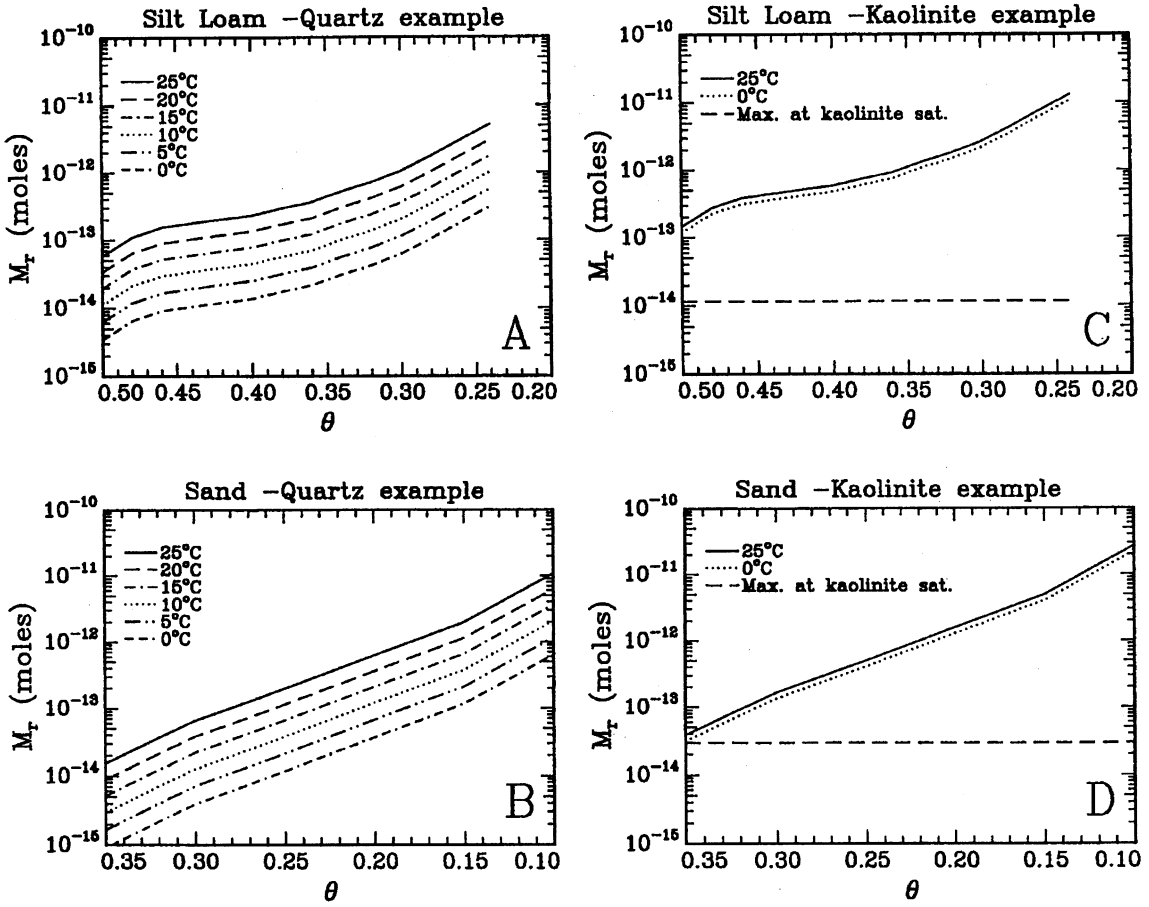

Fig. 7. Solute generated by pores that drain at the particular water content interval for a variety of temperature for the dissolution of quartz (silt loam and sand textural cases; A, B, respectively) and the dissolution of kaolinite (silt loam and sand textural classes; C, D, respectively). Calculated with Eqn. 14 assuming L = 100 cm, λ = 1 and an affinity of 1.

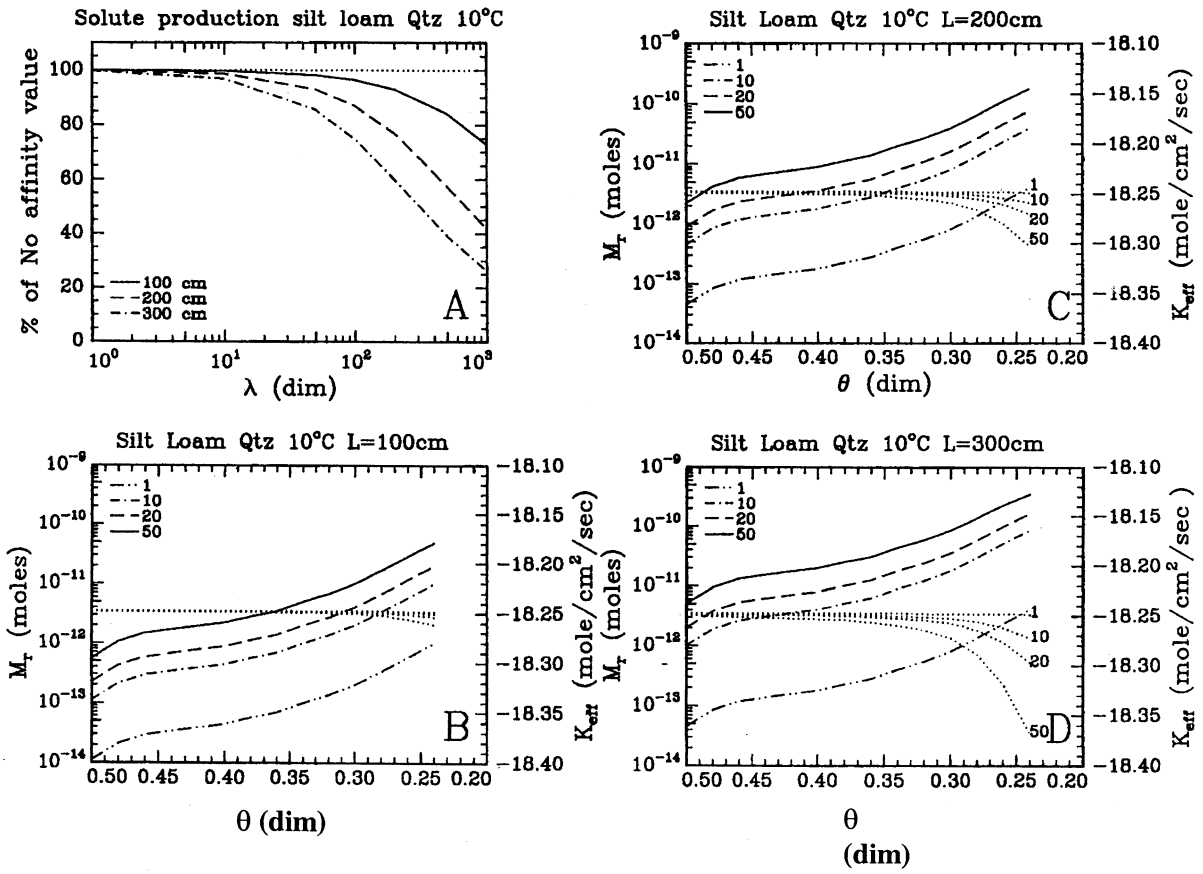

Fig. 8. Solute production expressed as a percentage of nonaffinity case solute production plotted against roughness for a variety of L (A). A value of 100% indicates that the model (with affinity) produced the same amount of solute as the same model without affinity. Notice that affinity becomes important (i.e., reduces solute production efficiency) for $\lambda > 50$ in the dissolution of quartz. Silica production by pores that drain at a particular water content for a temperature of 10°C, for A variety of λ; L = 100 (B), L = 200 (C), L = 300 (D). Calculations completed for the dissolution of quartz in the silt loam texture example. K_{eff} is the effective rate constant (see text).

the differences between the natural soils system, where packets of fluid are sometimes trapped in pores by matric forces, and reactor experiments, where fluid is moving efficiently overall grain surfaces. These systems are difficult to compare because it is difficult to compute a water residence time per unit surface area for the natural soil system.

The results of the temperature sensitivity analysis suggest that (holding other factors constant) the response of weathering to temperature changes will be smaller than is predicted by the Arrhenius equation with the appropriate laboratory activation energy. The reason for this is that temperature also influences the viscosity of water which in turn affects mineral-water contact time. An increase in temperature increases the rate of dissolution, but it also decreases soil-water residence time. Thus the extent of reaction is reduced somewhat.

The temperature effect on dynamic viscosity will hold true for all weathering reactions, and will reduce the temperature feedback on weathering as long as the pore water is not close to saturation. If that is the case we should see lower activation energies in field studies than in laboratory studies if the viscosity effect is not masked by other feedbacks. Recent field studies of albite weathering in which activation energies were actually calculated (Velbel, 1993b; White and Blum, 1995) and laboratory studies (Knauss and Wolery, 1986; Sverdrup, 1990; Hellman, 1994; Blum and Stillings, 1995; Chen and Brantley, 1997) allow the comparison to be made (Table 5). Table 5 shows some scatter, with silica release from albite dissolution having an activation energy 6 kJ/mole lower in the field than in the laboratory. For sodium release from albite dissolution, White and Blum's field energy is 6.3 kJ/mole lower than Hellman's (1994), while Velbel's (1993b) field derived activation energy was 7 kJ/mole higher. These discrepancies probably fall within the error of estimation (note the wide scatter of activation energies among the laboratory and field studies). Evaluating activation energies is problematic in the field, because it is difficult to find watersheds that are identical in every way except for temperature. It is interesting to note that studies by Bluth and Kump (1994) and Summerfield and Hulton (1994) failed to find a strong temperature dependence on weathering rates. There are many physical, chemical and biologic processes involved in soil weathering that are dependent on temperature which the model does not consider. Furthermore, it has been shown by White and Brantley (1995) that the activation energy of some weathering reactions is affected by pH, so the

Table 5. Activation energies calculated from laboratory and field studies.

Mineral	Field (kJ/mole)	Reference	Laboratory (kJ/mole)	Reference
Albite (Na release)	62.5	White and Blum (1995)	68.8 ± 4.5	Hellman (1994)
	77	Velbel (1993a)	67.7	Blum and Stillings (1995)
			64	Sverdrup (1990)
			54	Knauss and Wolery (1986)
Albite (Si release)	59.4	White and Blum (1995)	65.3 ± 3.3	Chen and Brantley (1997)

net effect of temperature on weathering probably varies from place to place.

Our model incorporates all the assumptions of the original Childs and Collis-George (1950) model. These include the assumption that the effective resistance of the pore to drainage is controlled by the surface tension forces acting on the smallest radius of the pore, and that water does not bypass narrow pores. Actual soil micropores are probably interconnected. Consequently, the notion that each class of micropore can be modeled as an isolated plug flow reactor is a simplification. Mixing of water and flushing of micropores by other micropores is certainly possible. However many field studies of water displacement in well structured soils (Quisenberry and Phillips, 1976, 1978; Priebe and Blackmer, 1989) show that very little displacement of water occurs, an observation that is attributed to the movement of water through pores without mixing. Other field studies show that antecedent moisture conditions can influence the degree of mixing in the soil (Parnell, 1993). For wetter antecedent moisture conditions, more mixing occurs. For drier antecedent moisture conditions, less mixing occurs and bypass flow is much more prevalent. The model is thus most applicable for drier conditions or well structured soils where dual porosity models are more appropriate. The model also does not treat the diffusion of solute from other micropores. These two limitations of the model (pore isolation and no diffusion) means that it will underestimate the leaching rate of the soil.

We assume in the model that surface tension forces are the dominant force holding water to the soil grains. This is accurate for the pores that are capable of draining by gravity (which have been shown to be the volumetrically largest contributor of water; Duguid and Lee, 1977; Shaffer et al., 1979; Watson and Luxmoore, 1986; Wilson and Luxmoore, 1988; Jabro et al., 1991b). Eqn. 16 suggests that the amount of solute contributed by each pore is dependent on L^3. The strong dependence on L makes the assumption that all of the pores have the same pore length tenuous, because minor variations of pore length will have a significant impact on solute accumulation. Jury et al. (1991) indicates that, to estimate unsaturated hydraulic conductivity correctly for some soil textures with the Childs and Collins-George model, smaller pores must be allowed to have longer pore lengths than larger micropores. Thus, assumption of uniform pore length will cause the model to underestimate the solute contributed by smaller pores. However, given these simplifications, our model still presents a tractable first attempt to conceptually investigate coupling between both fluid flow and kinetics in an unsaturated soil.

6. CONCLUSIONS

Field studies of soil water chemistry and soil structure suggest that a variety of weathering microenvironments exist within soils. These microenvironments are characterized by a wide range of rates of weathering, due to differences in specific surface area and water residence time. A simple plug-flow model has been developed to examine how temperature influences rates of weathering within these micropores and how temperature affects which microenvironments drain. The model suggests that the bulk of the weathering occurs in microenvironments characterized by smaller pores, where water residence times are long and specific areas are high. Since some of these environments cannot drain because of surface tension forces, diffusion of solute to microenvironments that do drain is an important mechanism in transferring solute out of a soil.

The feedback of temperature on weathering in a soil (holding other factors constant) should be weaker than what is predicted using the Arrhenius equation and a laboratory activation energy. A primary reason for this is the effect of temperature on water viscosity which will reduce water residence time as temperature is increased, and increase water residence time as temperature decreases. The temperature dependence of surface tension and water viscosity can be included in the Arrhenius equation by adjusting the laboratory-derived activation energy. Further work should incorporate other temperature dependent mechanisms in the model to see what the overall feedback of temperature is on weathering, and how this will vary spatially. We should also identify what portion of the matric potential water content curve dominates the chemistry of soil percolate and how this may vary with soil texture and season. This simple model provides a useful first approximation for coupling hydrologic and chemical processes in the continuum of pores that make up the natural soil system. We hope it will stimulate further research on the mechanisms that move water and solute from pore to pore and will enable us to identify the critical parts of the soil fabric that control watershed chemistry.

Acknowledgments—The core ideas of this paper were enhanced by a series of excellent lectures by Daniel Fritton, Penn State professor of agronomy. The authors would like to thank Susan Brantley for thoroughly reviewing previous drafts of the manuscript. The authors would also like to thank Michael Velbel and an anonymous reviewer for insightful comments. Support for this work was provided by a grant from NASA, through its Earth Observing System program.

Associate editor: M. Machesky

REFERENCES

Anbeek C. (1992) The dependence of dissolution rates on grainsize for some fresh and weathered feldspars. *Geochim. Cosmochim. Acta* **56**, 3957–3970.

Arthur M. A. and Fahey T. J. (1993) Controls of soil solution chemistry in a sub alpine forest in north-central Colorado. *Soil Sci. Soc. Am. J.* **57**, 1122–1130.

Baver L. D. (1938) Soil permeability in relation to non-capillary porosity. *Soil Sci. Soc. Am. J.* **2**, 52–56.

Berner R. A. and Berner E. K. (1997) Silicate weathering and climate. In *Tectonic Uplift and Climate Change* (ed. W. F. Ruddiman), pp. 353–365.

Beven K. and Germann P. (1981) Water flow in soil macropores 2: A combined flow model. *J. Soil Sci.* **32**, 15–29.

Beven K. and Germann P. (1982) Macropores and water flow in soils. *Water Resources Res.* **18**, 1311–1325.

Blum A. E. and Stillings L. L. (1995) Feldspar dissolution kinetics. In *Chemical Weathering Rates of Silicate Minerals*(eds. A. F. White and S. L. Brantley), pp. 291–351. Review 31. Mineral Society of America.

Bluth G. J. S. and Kump L. R. (1994) Lithologic and climatologic controls of river chemistry. *Geochim. Cosmochim. Acta* **58**, 2341–2359.

Bouma J. and Dekker L. W. (1978) A case study on infiltration into dry clay soil I: Morphological observations. *Geoderma* **20**, 41–51.

Bouma J., Jongerius O., Boersma A., Jager A., and Schoonderbeek D. (1977) The function of different types of macropores during saturated flow through four swelling horizons. *Soil Sci. Soc. Am. J.* **21**, 945–950.

Brady P. V. (1991) The effect of silicate weathering on global temperature and atmospheric CO_2. *J. Geophys. Res.* **96** *(B11)*, 18101–18106.

Brady P. V. and Carroll S. A. (1994) Direct effects of CO_2 and temperature on silicate weathering: Possible implications for climate control. *Geochim. Cosmochim. Acta* **58**, 1853–1858.

Brantley S. L. (1992) Kinetics of dissolution and precipitation: Experimental and field results. In *Proceedings of the 7th International Symposium on Water-Rock Interaction* (eds. Y. K. Kharaka and A. S. Maest). Park City, Utah pp. 3–6.

Burch T. E., Nagy K. L., and Lasaga A. C. (1993) Free energy dependence of albite dissolution kinetics at 80°C and pH 8.8. *Chem. Geol.* **105**, 137–162.

Campbell D. J., Kinniburgh D. G., and Beckett P. H. T. (1989) The soil solution chemistry of some Oxfordshire soils: Temporal and spatial variability. *J. Soil Sci.* **40**, 321–339.

Carroll S. A. and Walther J. V. (1990) Kaolinite dissolution at 25°, 60° and 80°. *Am. J. Sci.* **290**, 797–810.

Chahal R. (1965) The effect of temperature and trapped air on matric suction. *Soil Sci.* **100**, 262–266.

Chen Y. and Brantley S. L. (1997) Temperature- and pH-dependence of albite dissolution rate at acid pH. *Chem. Geol.* **135**, 275–290.

Childs E. C. (1964) A study of the movement of water through soil. *Endeavour* **23**, 81–84.

Childs E. C. and Collis-George N. (1950) The permeability of porous materials. *Proc. R. Soc. Lond. A* **201**, 392–405.

Chou L. and Wollast R. (1984) Study of the weathering of albite at room temperature and pressure with a fluidized bed reactor. *Geochim. Cosmochim. Acta* **48**, 2205–2217.

Cozarelli I. M., Hermann J. S., and Parnell R. A. (1987) The mobilization of aluminum in a natural soil system: Effects of hydrologic pathways. *Water Resources Res.* **23**, 859–874.

De Vries J. and Chow T. L. (1978) Hydrologic behavior of a forested mountain soil in coastal British Columbia. *Water Resources Res.* **14**, 935–942.

Denning A. S., Barron J., Mast M. A., Arthur M. (1991) Hydrologic pathways and chemical composition of runoff during snow melt in Loch Vale watershed Rocky Mountain National Park, Colorado, USA.

Drever J. I. (1994) The effect of land plants on weathering rates of silicate minerals. *Geochim. Cosmochim. Acta* **58**, 3209–3216.

Duguid J. O. and Lee P. C. Y. (1977) Flow in fractured porous media. *Water Resources Res.* **14**, 558–566.

Edmond J. M., Palmer M. R., Measures C. I., Grant B., and Stallard R. F. (1995) The fluvial geochemistry and denudation rate of the Guayana Shield in Venezuela Colombia, and Brazil. *Geochim. Cosmochim. Acta* **59**, 3301–3325.

Edmond J. M. and Huh Y. (1997) Chemical weathering yields from basement and Orogenic Terrains in Hot and Cold Climates. In *Tectonic Uplift and Climate Change* (ed. W. F. Ruddiman), pp. 329–351.

Flury M., Fluhler H., Jury W. A., and Levenberger J. (1994) Susceptibility of soils to preferential flow of water: A field study. *Water Resources Res.* **30**, 1945–1954.

Freeze A. C. and Cherry L. M. (1979) *Groundwater*. Prentice-Hall.

Gardner R. (1955) Relation of temperature to moisture tension of soil. *Soil Sci.* **79**, 257–265.

Germann P. and Beven K. (1981) Water flow in soil macropores 1: An experimental approach. *J. Soil Sci.* **32**, 1–13.

Giesler R. and Lundstrom U. (1993) Soil solution chemistry: Effects of bulking soil samples. *Soil Sci. Soc. Am. J.* **57**, 1283–1288.

Giesler R., Lundstrom U. S., and Grip H. (1996) Comparison of soil solution chemistry assessment using zero-tension lysimeters or centrifugation. *Eur. J. Soil Sci.* **47**, 395–405.

Grieve I. C. (1990) Soil and soil solution chemical composition at three sites within Loch Dee catchment, SW Scotland. *J. Soil Sci.* **41,** 269–277.

Haines W. B. (1927) Studies in the physical properties of soils: IV A further contribution to the theory of capillary phenomena in soil. *J. Agric. Sci.* **17**, 264–290.

Haines W. B. (1929) Studies in the physical properties of soils: V. The hysteresis effect in capillary properties, and the modes of moisture distribution associated therewith. *J. Agric. Sci.* **20**, 97–116.

Haines B. L., Waide J. B., and Todd R. L. (1982) Soil solution nutrient concentrations sampled with tension and zero-tension lysimeters: Report of discrepancies. *Soil Sci. Soc. Am. J.* **46**, 658–660.

Haridasan M. and Jensen R. D. (1972) Effect of temperature on pressure head-water content relationship and conductivity of two soils. *Soil Sci Soc. Am. Proc.* **36**, 703–708.

Helgeson H. C., Murphy W. M., and Aagaard P. (1984) Thermodynamic and kinetic constraints on reaction rates among minerals and aqueous solutions. II Rate constants, effective surface area and the hydrolysis of feldspar. *Geochim. Cosmochim. Acta* **48**, 2405–2432.

Hellman R. L. (1994) The albite-water system: Part I. The kinetics of dissolution as a function of pH at 100,200 and 300°C. *Geochim. Cosmochim. Acta* **58**, 595–611.

Hendershot W. H. and Courchense F. (1991) Comparison of soil solution chemistry in zero tension and ceramic-cup tension lysemeters. *J. Soil Sci.* **42**, 577–583.

Henninger D. L. (1972) Surface soil moisture within a watershed—Variations, factors influencing and relationship to runoff. M.A. thesis. The Pennsylvania State University.

Hopmans J. W. and Dane J. H. (1985) Effect of temperature-dependent hydraulic properties on soil water movement. *Soil Sci. Soc. Am. J.* **49**, 51–58.

Hopmans J. W. and Dane J. H. (1986) Temperature dependence of soil water retention curves. *Soil Sci. Soc. Am. J.* **50**, 562–567.

Horton J. H. and Hawkins R. H. (1965) Flow path of rain from the soil surface to the water table. *Soil Sci.* **100**, 377–383.

Jabro J. D., Fritton D. D., and Dobos R. R. (1991a) Spatial variability of field- saturated hydraulic conductivity in four central Pennsylvania soils. *Trends Soil Sci.* **1**, 253–269.

Jabro J. D., Lotse E. G., Simmons K. E., and Baker D. E. (1991b) A field study of macropore flow under saturated conditions using a bromide tracer. *J. Soil Water Conserv.* **46**, 376–380.

Johnson T. E. (1991) Stream flow sources and flow pathways in a forested headwater catchment. Ph.D. thesis. The Pennsylvania State University.

Jury W. A., Gardner W. R., and Gardner W. H. (1991) *Soil Physics.* 5th ed. Wiley.

Kazda M. and Katszensteiner K. (1993) Factors influencing the soil solution chemistry in Norway spruce stands in the Bohemian forest, Austria. *Agric. Ecosyst. Environ.* **47**, 135–145.

Knauss K. G. and Wolery T. J. (1986) Dependence of albite dissolution kinetics on pH and time at 25°C and 70°C. *Geochim. Cosmochim. Acta* **30**, 2481–2497.

Kump L., Brantley S. L., and Arthur M. A. (2000) Chemical weathering, atmospheric CO_2 and climates. *Earth, Planetary Sci. Rev.* **28**, 611–667.

Laidler K. J. (1987) *Chemical Kinetics.* 3rd ed. Harper and Row.

Lasaga A. C. (1981) Rate laws of chemical reactions. In *Kinetics of Geochemical Processes*, pp. 1–67. Reviews in Mineralogy 8. Mineralogical Society of America.

Lasaga A. C. (1984) Chemical kinetics of water-rock interactions. *J. Geophys. Res.* **89**, 4009–4025.

Lauren J. G., Wagenet R. J., Bouma J., and Wosten J. H. M. (1988) Variability of saturated hydraulic conductivity in a Glossaquic Hapludalf with macropores. *Soil Sci.* **145**, 20–28.

Ligon J. T., Wilson T. V., Allen J. F., and Singh V. P. (1980) Tracing vertical translocation of soil moisture. *J. Hydraulic Division Am. Soc. Civ. Eng.* **103,** *(HY10)*, 1147–1158.

Luxmoore R. J. (1980) Micro-, meso- and macroporosity of soil. *Soil Sci. Soc. Am. J.* **45**, 671.

Magid J. and Christensen N. (1993) Soil solution sampled with and without tension in Arable and Heathland soils. *Soil Soc. Sci. Am. J.* **57**, 1463–1469.

Marshall T. J. (1958) A relation between permeability and size distribution of pores. *J. Soil Sci.* **9**, 1–8.

Mercury L. and Tardy Y. (2001) Negative pressure of stretched liquid water. Geochemistry of soil capillaries. *Geochim. Cosmochim. Acta* **65**, 3391–3408.

Moulton K. L., West J., and Berner R. A. (2000) Solute flux and mineral mass balance approaches to the quantification of plant effects on silicate weathering. *Am. J. Sci.* **300**, 539–571.

Nagy K. L., Blum A. E., and Lasaga A. C. (1991) Dissolution and precipitation kinetics of kaolinite at 80°C and pH 3: The dependence on solution saturation state. *Am. J. Sci.* **291**, 649–686.

Nelson W. R. and Baver L. D. (1940) Movement of water through soils in relation to the nature of the pores. *Soil Sci. Soc. Am. Proc.* **4**, 69–76.

Nielsen D. R., Biggar J. W., and Erb K. T. (1973) Spatial variability of field-measured soil-water properties. *Hilgardia* **42**, 215–260.

Parnell R. A. (1993) Hydrologic control of chemical disequilibria in soil and surface waters, Sogndal, Norway. *Chem. Geol.* **105**, 101–115.

Peck A. J. (1960) Change of moisture tension with temperature and air pressure: Theoretical. *Soil Science.* **89**, 303–310.

Priebe D. L. and Blackmer A. M. (1989) Preferential movement of oxygen-18 labeled water and nitrogen-15 labeled urea through macropores in a Nicollet soil. *J. Environ. Qual.* **18**, 66–72.

Quisenberry V. L. and Phillips R. E. (1976) Percolation of surface-applied water in the field. *Soil Sci. Soc. Am. J.* **40**, 484–489.

Quisenberry V. L. and Phillips R. E. (1978) Displacement of soil water by simulated rainfall. *Soil Sci. Soc. Am. J.* **42**, 675–679.

Quisenberry V. L., Phillips R. E., and Zeleznik J. M. (1994) Spatial distribution of water and chloride macropore flow in a well structured soil. *Soil Sci. Soc. Am. J.* **58**, 1294–1300.

Richards L. A. and Weaver L. R. (1944) Moisture retention by some irrigated soils as related to soil-moisture tension. *J. Agric. Res.* **69**, 215–235.

Richter G. and Jury W. A. (1986) A microlysimeter field study of solute transport through a structured sandy loam soil. *Soil Sci Soc. Am. J.* **50**, 863–868.

Rimstidt J. D. and Barnes H. L. (1980) The kinetics of silica-water reactions. *Geochim. Cosmochim. Acta* **44**, 1683–1699.

Rogowski A. S., Engman E. T., and Jacoby E. L. (1974) Transient response of a layered, sloping soil to natural rainfall in the presence of a shallow water table: Experimental results. Contribution of the USDA-ARS (ARS NE 30).

Russell A. E. and Ewel J. J. (1985) Leaching from a tropical andept during big storms: A comparison of three methods. *Soil Sci.* **139**, 181–189.

Schoeneberger P. and Amoozegar A. (1990) Directional saturated hydraulic conductivity and macropore morphology of a soil-saprolite sequence. *Geoderma* **46**, 31–49.

Shaffer K. A., Fritton D. D., and Baker D. E. (1979) Drainage water sampling in a wet, dual-pore soil system. *J. Environ. Qual.* **8**, 241–246.

Stallman R. W. (1964) Multi phase fluids in porous media: A review of theories pertinent to Hydrologic Studies. Fluid movement in Earth materials. USAS Prof. Paper 411-E, United States Government Printing Office.

Starr M. R. (1985) Variation in the quality of tension lysimeter soil water samples from a Finish forest soil. *Soil Sci.* **140**, 453–461.

Stumm W. and Morgan J. (1982) *Aquatic Chemistry.* 2nd ed. Wiley.

Summerfield M. A. and Hulton N. J. (1994) Natural controls of fluvial denudation rates in major world drainage basins. *J. Geophys. Res.* **99**, 13,871–13,883.

Sverdrup H. U. (1990) *The Kinetics of Base Cation Release Due to Chemical Weathering.* Lund University Press.

Swistock B. R., Yamona J. J., Dewalle D. R., and Sharpe W. E. (1990) Comparison of soil water chemistry and sample size requirements for pan versus. tension lysimeters. *Water Air Soil Pollut.* **50**, 387–396.

Swoboda-Coburg N. G. and Drever J. I. (1993) Mineral dissolution rates in plot scale field and laboratory experiments. *Chem. Geol.* **105**, 51–69.

Thomas G. W. and Phillips R. E. (1979) Consequences of water movement in macropores. *J. Environ. Qual.* **8**, 149–152.

Ugolini F. C., Dahlgren R., Shoji S., and Ito T. (1988) An example of andosolization and podzolization as revealed by soil solution studies, Southern Hakkoda Northeastern Japan. *Soil Sci.* **145**, 111–125.

Velbel M. A. (1990) Influence of temperature and mineral surface characteristics on feldspar weathering. *Water Resources Res.* **26**, 3049–3053.

Velbel M. A. (1993a) Constancy of silicate-mineral weathering-rate ratios between natural and experimental weathering: Implications for hydrologic control of differences in absolute rates. *Chem. Geol.* **105**, 89–99.

Velbel M. A. (1993b) Temperature dependance of silicate weathering in nature: How strong a negative feedback on long term accumulation of atmospheric CO2 and global greenhouse warming. *Geology* **21**, 1059–1062.

Volk T. (1987) Feedbacks between weathering and atmospheric CO_2 over the last 100 million years. *Am. J. Sci.* **287**, 763–779.

Volk T. (1989) Rise of angiosperms as a factor in long-term climatic cooling. *Geology* **17**, 107–110.

Watson K. W. and Luxmoore R. J. (1986) Estimating macroporosity in a forested watershed by use of a tension lysimeter. *Soil Sci. Soc. Am. J.* **50**, 141–159.

Weast L. and Melvin J. A. (1979) *CRC Handbook of Chemistry and Physics.* CRC Press.

White A. F. and Petersen M. L. (1990) Role of reactive surface area characterization in geochemical kinetic models. In *Chemical Modeling in Aqueous Systems 2* (eds. D. L. Melchior and R. L. Bassett), pp. 461–475. Symposium Series No. 416. ACS.

White A. F. and Blum A. E. (1995) Effects of climate on chemical weathering in watersheds. *Geochim. Cosmochim. Acta* **59**, 1729–1747.

White A. F. and Brantley S. L. (1995) Chemical weathering rates of silicate minerals: An overview. In *Chemical Weathering Rates of Silicate Minerals*(eds. A. F. White and S. L. Brantley), pp. 1–22. Review 31. Mineral Society of America.

Wilkinson G. E. and Klute A. (1962) The temperature effect on the equilibrium energy status of water held by porous media. *Soil Sci. Soc. Proc.* **26**, 326–329.

Wilson G. V. and Luxmoore R. J. (1988) Infiltration, macroporosity, and mesoporosity distributions on two forested watersheds. *Soil Sci. Soc. Am. J.* **52**, 329–335.

Wilson G. V., Jardine D. M., Luxmoore R. J., and Jones J. R. (1990) Hydrology of a forested hillslope during storm events. *Geoderma* **46**, 119–138.

Zabowski D. and Ugolini F. C. (1990) Lysimeter and centrifuge soil solutions: Seasonal differences between methods. *Soil Sci. Soc. Am. J.* **54**, 1130–1135.

Zabowski D. and Ugolini F. C. (1992) Seasonality in the mineral stability of a sub alpine spodosol. *Soil Sci.* **154**, 497–507.